

LEARNING INVARIANTS THROUGH SOFT UNIFICATION

Nuri Cingillioglu

Department of Computing
Imperial College London
nuric@imperial.ac.uk

Alessandra Russo

Department of Computing
Imperial College London
a.russo@imperial.ac.uk

ABSTRACT

Human reasoning involves recognising common underlying principles across many examples by utilising variables. The by-products of such reasoning are invariants that capture patterns across examples such as “if someone went somewhere then they are there” without mentioning specific people or places. Humans learn what variables are and how to use them at a young age, and the question this paper addresses is whether machines can also learn and use variables solely from examples without requiring human pre-engineering. We propose Unification Networks that incorporate soft unification into neural networks to learn variables and by doing so lift examples into invariants that can then be used to solve a given task. We evaluate our approach on four datasets to demonstrate that learning invariants captures patterns in the data and can improve performance over baselines.

1 INTRODUCTION

Humans have the ability to process symbolic knowledge and maintain symbolic thought (Unger & Deacon, 1998). When reasoning, humans do not require combinatorial enumeration of examples but instead utilise invariant patterns with placeholders replacing specific entities. Symbolic cognitive models (Lewis, 1999) embrace this perspective with the human mind seen as an information processing system operating on formal symbols such as reading a stream of tokens in natural language. The language of thought hypothesis (Morton & Fodor, 1978) frames human thought as a structural construct with varying sub-components such as “X went to Y”. By recognising what varies across examples, humans are capable of lifting examples into invariant principles that account for other instances. This symbolic thought with variables is learned at a young age through symbolic play (Piaget, 2001). For instance a child learns that a sword can be substituted with a stick (Frost et al., 2004) and engage in pretend play.

Although variables are inherent in models of computation and symbolic formalisms, as in first-order logic (Russell & Norvig, 2016), they are pre-engineered and used to solve specific tasks by means of unification or assignments that bound variables to given values. However, when learning from data only, being able to recognise when and which symbols should take on different values, i.e. symbols that can act as variables, is crucial for lifting examples into general principles that are invariant across multiple instances. Figure 1 shows the invariant learned by our approach: if someone is the same thing as someone else then they have the same colour. With this invariant, our approach can solve *all* of the training and test examples in task 16 of the bAbI dataset (Weston et al., 2016).

In this paper we address the question of whether a machine can learn and use the notion of a *variable*, i.e. a symbol that can take on different values. For instance, given an example of the form “bernhard is a frog” the machine would learn that the token “bernhard” could be *someone* else and the token “frog” could be *something* else. If we consider unification a selection of the most appropriate value for a variable given a choice of values, we can reframe it as a form of attention. Attention models (Bahdanau et al., 2015; Luong et al., 2015; Chaudhari et al., 2019) allow neural networks to focus, attend to certain parts of the input often for the purpose of

$$X:\text{bernhard is a } Y:\text{frog}$$

$$Z:\text{lily is a } Y:\text{frog}$$

$$Z:\text{lily is } A:\text{green}$$

$$\text{what colour is } X:\text{bernhard}$$

$$A:\text{green}$$

Figure 1: Invariant learned for bAbI task 16, basic induction, where $X:\text{bernhard}$ denotes a variable with default symbol bernhard. This single invariant accounts for all the training and test examples.

selecting a relevant portion. Since attention mechanisms are also differentiable they are often jointly learned within a task. This perspective motivates our idea of a unification mechanism that utilises attention and is therefore fully differentiable which we refer to as *soft unification*.

Hence, we propose an end-to-end differentiable neural network approach for learning and utilising the notion of a variable that in return can lift examples into invariants used by the network to perform reasoning tasks. Specifically, we (i) propose a novel architecture capable of learning and using variables by lifting a given example through soft unification, (ii) present the empirical results of our approach on four datasets and (iii) analyse the learned invariants that capture the underlying patterns present in the tasks. Our implementation using Chainer (Tokui et al., 2015) is publicly available at <https://github.com/nuric/softuni> with the accompanying data.

2 SOFT UNIFICATION

Reasoning with variables involves identifying what variables are, the setting in which they are used as well as the process by which they are assigned values. When the varying components, i.e. variables, of an example are identified, the remaining structure can be lifted into an invariant which then accounts for multiple other instances.

Definition 1 (Variable). Given a set of symbols \mathbb{S} , a variable \mathbf{X} is defined as a pair $\mathbf{X} \triangleq (x, s_d)$ where $s_d \in \mathbb{S}$ is the *default symbol* of the variable and x is a discrete random variable of which the support is \mathbb{S} . The representation of a variable $\phi(\mathbf{X};s_d)$ is equal to the expected value of the corresponding random variable x given the default symbol s_d :

$$\phi(\mathbf{X};s_d) = \mathbb{E}_{x \sim P}[\phi(x)] = \sum_{x \in \mathbb{S}} P(x = x|s_d)\phi(x) \quad (1)$$

where $\phi : \mathbb{S} \rightarrow \mathbb{R}^d$ is a d -dimensional real-valued feature of a symbol s .

For example, ϕ could be an embedding and $\phi(\mathbf{X};s_d)$ would become a weighted sum of symbol embeddings as in conventional attention models. The default symbol of a variable is intended to capture the variable’s bound *meaning* following the idea of referants by Frege (1948). We denote variables using $\mathbf{X}, \mathbf{Y}, \mathbf{A}$ etc. such as $\mathbf{X}:\text{bernhard}$ where \mathbf{X} is the name of the variable and *bernhard* the default symbol as shown in Figure 1.

Definition 2 (Invariant). Given a structure (e.g. list, grid) \mathcal{G} over \mathbb{S} , an invariant is a pair $I \triangleq (G, \psi)$ where $G \in \mathcal{G}$ is the invariant example such as a tokenised story and $\psi : \mathbb{S} \rightarrow [0, 1]$ is a function representing the degree to which the symbol is considered a variable. Thus, the final representation of a symbol s included in G , $\phi_I(s)$ is:

$$\phi_I(s) = (1 - \psi(s))\phi(s) + \psi(s)\phi(\mathbf{X};s) \quad (2)$$

the linear interpolation between its representation $\phi(s)$ and its variable bound value with itself as the default symbol $\phi(\mathbf{X};s)$.

We adhere to the term invariant and refrain from mentioning rules, unground rules, etc. used in logic-based formalisms, e.g. Muggleton & de Raedt (1994), since neither the invariant structure needs to be rule-like nor the variables carry logical semantics. This distinction is clarified in Section 6.

Definition 3 (Unification). Given an invariant I and an example $K \in \mathcal{G}$, unification binds the variables in I to symbols in K . Defined as a function $g : \mathcal{I} \times \mathcal{G} \rightarrow \mathcal{G}$, unification binds variables by computing the probability mass functions, P in equation 1, and returns the unified representation using equation 2. The probability mass function of a variable $\mathbf{X};s_d$ is:

$$P(x = x|s_d) = \text{softmax}(\phi_U(s_d)\phi_U(K)^T), \quad K = \text{support of } x \quad (3)$$

where $\phi_U : \mathbb{S} \rightarrow \mathbb{R}^d$ is the unifying feature of a symbol and $\phi_U(K) \in \mathbb{R}^{|\mathbb{S}| \times d}$ is applied element wise to symbols in K . If g is differentiable, it is referred to as soft unification.

We distinguish ϕ from ϕ_U to emphasise that the unifying properties of the symbols might be different from their representations. For example, $\phi(\text{bernhard})$ could represent a specific person whereas $\phi_U(\text{bernhard})$ the notion of *someone*.

Overall soft unification incorporates 3 learnable components: ϕ, ψ, ϕ_U which denote the base features, variableness and unifying features of a symbol respectively. Given an upstream, potentially task specific, network $f : \mathcal{G} \rightarrow \mathbb{S}$, an invariant $I \in \mathcal{I}$ and an input example $K \in \mathcal{G}$ with a corresponding desired output $a \in \mathbb{S}$, the following holds:

$$f \circ g(I, K) = f(K) = a \tag{4}$$

where f now predicts based on the unified representation produced by g . In this work, we focus on g , the invariants it produces together with the interaction of $f \circ g$.

3 UNIFICATION NETWORKS

Since soft unification is end-to-end differentiable, it can be incorporated into existing task-specific upstream architectures. We present 3 architectures that model $f \circ g$ using multi-layer perceptrons (MLP), convolutional neural networks (CNN) and memory networks (Weston et al., 2015) to demonstrate the flexibility of our approach. In all cases, the d dimensional representation of symbols are learnable embeddings $\phi(s) = O[s]^T \mathbf{E}$ with $\mathbf{E} \in \mathbb{R}^{|\mathbb{S}| \times d}$ randomly initialised by $\mathcal{N}(0, 1)$ and $O[s]$ the one-hot encoding of the symbol. The variableness of symbols is a learnable weight $\psi_w(s) = \sigma(w_s)$ where $w \in \mathbb{R}^{|\mathbb{S}|}$ and σ is the sigmoid function. We consider every symbol independently a variable irrespective of its surrounding context and leave further contextualised formulations as future work. The underlying intuition of this configuration is that a *useful* symbol for a correct prediction might need to take on other values for different inputs. This usefulness can be viewed as the inbound gradient to the corresponding w_s parameter and $\psi_w(s)$ acting as a gate. For further model details including the size of the embeddings, please refer to Appendix A.

Unification MLP (UMLP) (f : MLP, g : RNN) We combine soft unification into a multi-layer perceptron to process fixed length inputs. In this case, the structure \mathcal{G} is a sequence of symbols with a fixed length l , e.g. a sequence of digits 4234. Given an embedded input $\phi(\mathbf{k}) \in \mathbb{R}^{l \times d}$, the upstream MLP computes the output symbol based on the flattened representations $f(\phi(\mathbf{k})) = \text{softmax}(\mathbf{h}\mathbf{E}^T)$ where $\mathbf{h} \in \mathbb{R}^d$ is the output of the last layer. However, to compute the unifying features ϕ_U , definition 3, g uses a bi-directional GRU (Cho et al., 2014) running over $\phi(\mathbf{k})$ such that $\phi_U(k) = \mathbf{W}_U \Phi(k)$ where $\Phi(k) \in \mathbb{R}^d$ is the hidden state of the GRU at symbol k and $\mathbf{W}_U \in \mathbb{R}^{d \times d}$ is a learnable parameter. This model emphasises the flexibility around the boundary of $f \circ g$ and that the unifying features can be computed in any differentiable manner.

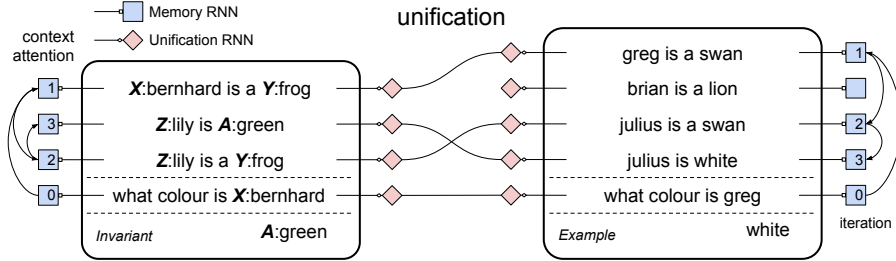


Figure 2: Graphical overview of soft unification within a memory network. Each sentence is processed by two bi-directional RNNs for memory and unification. At each iteration the context attention selects which sentences to unify and the invariant produces the same answer as the example.

Unification CNN (UCNN) (f : CNN, g : CNN) Given a grid of embedded symbols $\phi(\mathbf{K}) \in \mathbb{R}^{w \times h \times d}$ where w is the width and h the height, we use a convolutional neural network such that the final prediction is $f(\phi(\mathbf{K})) = \text{softmax}((\mathbf{W}\mathbf{h} + \mathbf{b})\mathbf{E}^T)$ where \mathbf{h} this time is the result of global max pooling and \mathbf{W}, \mathbf{b} are learnable parameters. We also model g using a *separate* convolutional network with the same architecture as f and set $\phi_U(k) = c_2(\text{relu}(c_1(k)))$ where c_1, c_2 are the convolutional layers. The grid is padded with 0s to obtain $w \times h \times d$ after each convolution such that every symbol has a unifying feature. This model conveys how soft unification can be adapted to the specifics of the domain for example by using a convolution in a spatially structured input.

Unification Memory Networks (UMN) (f : MemNN, g : RNN) Soft unification does not need to happen prior to f in a $f \circ g$ fashion but can also be incorporated at any intermediate stage multiple

Table 1: Sample context, query and answer triples and their training sizes *per task*. For distribution of generated number of examples per task on Sequence and Grid data refer to Appendix B.

Dataset	Context	Query	Answer	Training Size
Sequence	8384	duplicate	8	$\leq 1k, \leq 50$
Grid	$\begin{matrix} 0 & 0 & 3 \\ 0 & 1 & 6 \\ 8 & 5 & 7 \end{matrix}$	corner	7	$\leq 1k, \leq 50$
bAbI	Mary went to the kitchen. Sandra journeyed to the garden.	Where is Mary?	kitchen	1k, 50
Logic	$\begin{matrix} p(X) \leftarrow q(X). \\ q(a). \end{matrix}$	p(a).	True	1k, 10k, 50

times. To demonstrate this ability, we unify the symbols at different memory locations at each iteration of a Memory Network (Weston et al., 2015). Memory networks can handle a list of lists structure such as a tokenised story as shown in Figure 2. The memory network f uses the final hidden state of a bi-directional GRU (outer squares in Figure 2) as the sentence representations to compute a context attention. At each iteration, we unify the words between the attended sentences using the same approach in UMLP with another bi-directional GRU (inner diamonds in Figure 2) for unifying features $\phi_U(\text{bernhard}) = \mathbf{W}_U \Phi(\text{bernhard})$. Following equation 2, the new unified representation of the memory slot is computed and f uses it to perform the next iteration. Concretely, g produces an unification tensor $\mathbf{U} \in \mathbb{R}^{M \times m \times N \times d}$ where M and m is the number of sentences and words in the invariant respectively, and N is the number of sentences in the example such that after the context attentions are applied over M and N , we obtain $\phi(\mathbf{k}) \in \mathbb{R}^{m \times d}$ as the unified sentence at that iteration. Note that unlike in the UMLP case, the sentences can be of varying length. The prediction is then $\text{softmax}(\mathbf{W} \mathbf{h}_I^J + \mathbf{b})$ where \mathbf{h}_I^J is the hidden state of the invariant after J iterations. This setup, however, requires pre-training f such that the context attentions match the correct sentences.

A task might contain different questions such as “Where is X?” and “Why did X go to Y?”. To let the models differentiate between questions and potentially learn different invariants, we extend them with a repository of invariants $I \in \mathbb{I}$ and aggregate the predictions from each invariant. One simple approach is to sum the predictions of the invariants $\sum_{I \in \mathbb{I}} f \circ g(I, K)$ used in UMLP and UCNN. Another approach could be to use features from the invariants such as memory representations in the case of UMN. For UMN, we weigh the predictions using a bilinear attention η based on the hidden states at the first iteration \mathbf{h}_I^0 and \mathbf{h}_K^0 such that $\eta = \text{softmax}(\mathbf{h}_I^0 \mathbf{W} \mathbf{h}_K^{0T})$. To initially form the repository of invariants, we use the bag-of-words representation of the questions and find the most dissimilar ones based on their cosine similarity as a heuristic to obtain varied examples.

4 DATASETS

We use 4 datasets consisting of context, query and an answer (C, q, a) : fixed length sequences of symbols, shapes of symbols in a grid, story based natural language reasoning with the bAbI (Weston et al., 2016) dataset and logical reasoning represented as logic programs, examples shown in Table 1 with further samples in Appendix B. In each case we use an appropriate model: UMLP for fixed length sequences, UCNN for grid and UMN for iterative reasoning. We use synthetic datasets of which the data generating distributions are known to evaluate not only the quantitative performance but also the quality of the invariants learned by our approach.

Fixed Length Sequences We generate sequences of length $l = 4$ with 8 unique symbols represented as digits to predict (i) a constant, (ii) the head of the sequence, (iii) the tail and (iv) the duplicate symbol. We randomly generate 1000 triples and then only take the unique ones to ensure the test split contains unseen examples. The training is then performed over a 5-fold cross-validation.

Grid To spatially organise symbols, we generate a grid of size 3×3 with 8 unique symbols organised into 2×2 box of identical symbol, a vertical, diagonal or horizontal sequence of length 3, a cross or a plus shape and a triangle. In each task we predict (i) the identical symbol, (ii) the head of the sequence, (iii) the centre of the cross or plus and (iv) the corner of the triangle respectively. We follow the same procedure from sequences and randomly generate 1000 discarding duplicate triples.

bAbI The bAbI dataset has become a standard benchmark for evaluating memory based networks. It consists of 20 synthetically generated natural language reasoning tasks (refer to Weston et al. (2016) for task details). We take the 1k English set and use 0.1 of the training set as validation. Each token is lower cased and considered a unique symbol. Following previous works (Seo et al., 2017; Sukhbaatar et al., 2015), we take multiple word answers also to be a unique symbol in \mathbb{S} .

Logical Reasoning To demonstrate the flexibility of our approach and distinguish our notion of a variable from that used in logic based formalisms, we generate logical reasoning tasks in the form of logic programs using the procedure by Cingillioglu & Russo (2019). The tasks involve learning $f(C, Q) = \text{True} \leftrightarrow C \vdash Q$ over 12 classes of logic programs exhibiting varying paradigms of logical reasoning including negation by failure (Clark, 1978). We generate 1k and 10k logic programs per task for training with 0.1 as validation and another 1k for testing. We set the arity of literals to 1 or 2 using one random character from the English alphabet for predicates *and* constants, e.g. $p(p)$ and an upper case character for logical variables, e.g. $p(X)$.

5 EXPERIMENTS

We probe three aspects of soft unification: the impact of unification on performance over unseen data, the effect of multiple invariants and data efficiency. To that end, we train UMLP and UCNN with and without unification, UMN with pre-training using 1 or 3 invariants over either the entire training set or only 50 examples. Every model is trained 3 times via back-propagation using Adam (Kingma & Ba, 2015) on an Intel Core i7-6700 CPU using the following objective function:

$$J = \lambda_K \mathcal{L}_{\text{nl}}(f(K), a) + \lambda_U \left[\mathcal{L}_{\text{nl}}(f \circ g(I, K), a) + \tau \sum_{s \in \mathbb{S}} \psi_w(s) \right] \quad (5)$$

where \mathcal{L}_{nl} is the negative log-likelihood with sparsity regularisation over ψ at $\tau = 0.1$ to discourage the models from utilising spurious number of variables. For UMLP and UCNN, we set $\lambda_K = 0$, $\lambda_U = 1$ for training just the unified output and the converse for the non-unifying versions. To pre-train the UMN, we start with $\lambda_K = 1$, $\lambda_U = 0$ for 40 epochs then set $\lambda_U = 1$ to jointly train the unified output. For iterative tasks, the mean squared error between hidden states $(\mathbf{h}_I^j - \mathbf{h}_K^j)^2$ at each iteration j and, in the strongly supervised cases, the negative log-likelihood for the context attentions are also added to the objective function. Further details such as batch size and total number of epochs are available in Appendix C.

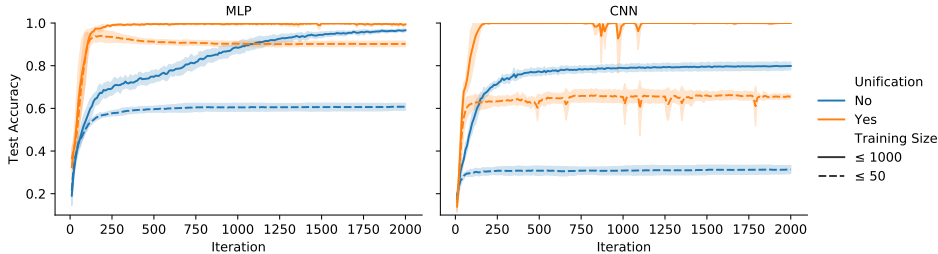


Figure 3: Test accuracy over iterations for Unification MLP and Unification CNN models with 1 invariant versus no unification. We observe that with soft unification the models achieve higher accuracy with fewer iterations than their plain counterparts on both per task training sizes.

Figure 3 portrays how soft unification generalises better to unseen examples in test sets - the same sequence or grid never appears in both the training and test sets as outlined in Section 4 - over plain models. Despite $f \circ g$ having more trainable parameters than f alone, the models with unification not only maintain higher accuracy in each iteration and solve the tasks in as few as 250 iterations with ≤ 1000 training examples but also improve accuracy by ≈ 0.3 when trained with only ≤ 50 per task. We believe soft unification architecturally biases the models towards learning structural patterns which in return achieves better results on recognising common patterns of symbols across examples. Results with multiple invariants are identical and the models seem to ignore the extra invariants due to the fact that the tasks can be solved with a single invariant and the regularisation applied on ψ zeroing out unnecessary invariants; further results in Appendix D. The fluctuations in

accuracy around iterations 750 to 1000 in UCNN are also caused by penalising ψ which forces the model to relearn the task with less variables half way through training.

Table 2: Aggregate error rates (%) on bAbI 1k for UMN and N2N, GN2N, MemNN by Sukhbaatar et al. (2015), Liu & Perez (2017) and Weston et al. (2015) respectively. Full comparison on individual tasks are available in Appendix D.

Training Size Supervision # Invs / Model	1k					1k				
	Weak		Strong			Weak				Strong
	1	3	1	3	3	N2N	GN2N	EntNet	QRN	MemNN
Mean	19.1	20.5	6.3	6.0	27.6	13.9	12.7	29.6	11.3	6.7
# > 5%	8	10	4	4	17	11	10	15	5	4

Following Tables 2 and 3, we observe a trend of better performance through strong supervision, more data per task and using only 1 invariant. We believe strong supervision aids with selecting the correct sentences to unify and in a weak setting the model attempts to unify arbitrary context sentences often failing to follow the iterative reasoning chain. The increase in performance with more data and strong supervision is consistent with previous work reflecting how $f \circ g$ can be bounded by the efficacy of f modelled as a memory network. As a result, only in the supervised case do we observe a minor improvement over MemNN by 0.7 in Table 2 and no improvement in the weak case over DMN or IMA in Table 3 with failing 17/20 and 12/12 tasks when trained using only 50 examples. The increase in error rate with 3 invariants, we speculate, stems from having more parameters and more pathways in the model rendering training more difficult.

Table 3: Aggregate task error rates (%) on the logical reasoning dataset for UMN and DMN, IMA by Cingillioglu & Russo (2019). Strong supervision, more data and only 1 invariant seem to improve the performance of UMN over plain iterative models. Individual task results are in Appendix D.

Training Size Supervision Arity # Invs / Model	1k				10k						50		20k	
	Weak		Strong		Weak		Strong						Weak	
	1	2	1	2	1	2	1	2	2	2	2	2	2	2
	1	3	1	3	1	3	1	1	3	3	3	DMN	IMA	
Mean	36.4	39.3	14.3	28.9	21.5	31.8	2.4	12.2	16.0	47.1	12	21.2	9.1	
# > 5%	9	11	7	11	7	10	1	5	9	12	12	11	5	

6 ANALYSIS

After training, we can extract the learned invariants by applying a threshold on $\forall s \in \mathbb{S} : \psi(s) > t$ indicating whether a symbol is used as a variable or not. We set $t = 0.0$ for all datasets except for bAbI, we use $t = 0.1$. The magnitude of this threshold seems to depend on the amount of regularisation τ , equation 5, and the number of training steps along with batch size all controlling how much ψ is pushed towards 0. Sample invariants shown in Figure 4 describe the common patterns present in the tasks with parts that contribute towards the final answer becoming variables. Extra symbols such as `is` or `travelled` do not emerge as variables, as shown in Figure 4a; we attribute this behaviour to the fact that changing the token `travelled` to `went` does not influence the prediction but changing the action, the value of `Z:left` to ‘picked’ does. However, based on random initialisation, our approach can convert a random symbol into a variable and let f compensate for the unifications it produces. For example, the invariant “`X:8 5 2 2`” could predict the tail of another example by unifying the head with the tail using ϕ_U , equation 3, of those symbols. Pre-training f as done in UMN seems to produce more robust and consistent invariants compared to immediately training $f \circ g$ since, we speculate, by equation 4 f might encourage $g(I, K) \approx K$.

Interpretability versus Ability A desired property of interpretable models is transparency (Lipton, 2018). A novel outcome of the learned invariants in our approach is that they provide an approximation of the underlying general principle present in the *data* such as the structure of multi-hop reasoning shown in Figure 4e. However, certain aspects such as temporal reasoning are still hidden inside f . In Figure 4b, although we observe `Z:morning` as a variable, the overall learned invariant captures nothing about how changing the value of `Z:morning` alters the behaviour of f . The model might look *before* or *after* a certain time point `X:bill` went somewhere depending what `Z:morning`

Y:john Z:left the X:football
 Y:john travelled to the A:office
 where is the X:football
 A:office

this Z:morning X:bill went to the Y:school
 yesterday X:bill journeyed to the A:park
 where was X:bill before the Y:school
 A:park

(a) bAbI task 2, two supporting facts. The model also learns Z:left since people can also drop or pick up objects potentially affecting the answer.

(b) bAbI task 14, time reasoning. X:bill and Y:school are recognised as variables alongside Z:morning capturing when someone went which is crucial to this task.

5 8 6 4 const 2
 X:8 3 3 1 head X:8
 8 3 1 Y:5 tail Y:5
 Z:1 4 3 Z:1 dup Z:1

0 X X 0 1 0 0 0 1
 0 X X 6 Y 8 0 5 4
 0 0 0 0 7 0 7 8 X
 box centre corner

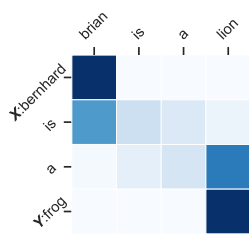
X:i (T) ← Z:l (T),
 Z:l (U) ← R:x (U),
 R:x (K) ← S:n (K),
 S:n (Y:o) ⊢ X:i (Y:o)

(c) Successful invariants learned with UMLP using 50 training examples only shown as (C, Q, a).

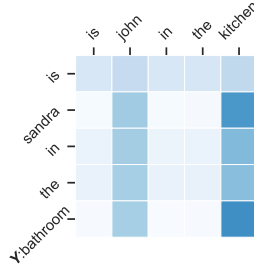
(d) Successful invariants learned with UCNN. Variable default symbols are omitted for clarity.

(e) Logical reasoning task 5 with arity 1. The model captures how S:n could entail X:i in a chain.

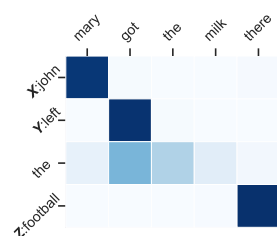
Figure 4: Invariants learned across the four datasets using the three architectures. For iterative reasoning datasets, bAbI and logical reasoning, they are taken from strongly supervised UMN.



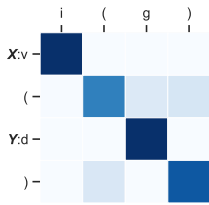
(a) bAbI task 16. A one-to-one mapping is created between variables X:bernhard with brian and Y:frog with lion.



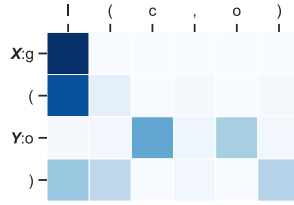
(b) bAbI task 6. Only Y:bathroom is recognised as variable creating a one-to-many binding to capture the same information.



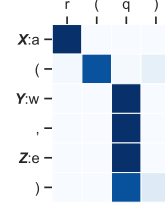
(c) bAbI task 2. When a variable is unused in the next iteration, e.g. Z:football, it unifies with random tokens often biased by position.



(d) Logical reasoning task 1. A one-to-one alignment is created between predicates and constants.



(e) Logical reasoning task 3. Arity 1 atom forced to bind with arity 2 creates a one-to-many mapping.



(f) Logical reasoning task 1. An arity 2 atom forced to bind with arity 1 creates a many-to-one mapping.

Figure 5: Variable assignment maps from equation 3. Darker cells indicate higher attention values.

binds to. Without the regularising term on $\psi(s)$, we initially noticed the models using, one might call extra, symbols as variables and binding them to the same value occasionally producing unifications such as “bathroom bathroom to the bathroom” and still f predicting, perhaps unsurprisingly, the correct answer as bathroom. Hence, regularising ψ with the correct amount τ in equation 5 seems critical in extracting not just any invariant but one that represents the common structure.

Soft unification from equation 3 reveals three main patterns: one-to-one, one-to-many or many-to-one bindings as shown in Figure 5. Figures 5a and 5d capture what one might expect unification to look where variables unify with their corresponding counterparts. However, occasionally the model can optimise to use less variables and *squeeze* the required information into a single variable, for example by binding Y:bathroom to john and kitchen as in Figure 5b. We believe this occurs due to

the sparsity constraint on $\psi(s)$ encouraging the model to be as conservative as possible. In a similar fashion, the unification can bind a single variable $Y:o$ to both other constants as in Figure 5e. Finally, if there are more variables than needed as in Figure 5f, we observe a many-to-one binding with $Y:w$ and $Z:e$ mapping to the same constant. This behaviour begs the question how does the model differentiate between $p(q)$ and $p(q, q)$. We speculate the model uses the magnitude of $\psi(w) = 0.037$ and $\psi(e) = 0.042$ to encode the difference despite both variables unifying with the same constant.

7 RELATED WORK

Learning an underlying general principle in the form of an invariant is often the means for arguing generalisation in neural networks. For example, Neural Turing Machines (Graves et al., 2014) are tested on previously unseen sequences to support the view that the model might have captured the underlying pattern or algorithm. In fact, Weston et al. (2015) claim “MemNNs can discover simple linguistic patterns based on verbal forms such as (X, dropped, Y), (X, took, Y) or (X, journeyed to, Y) and can successfully generalise the meaning of their instantiations.” However, this claim is based on the output of f and unfortunately it is unknown whether the model has truly learned such a representation or indeed is utilising it. Our approach sheds light to this ambiguity and presents these linguistic patterns explicitly as invariants ensuring their utility through g without solely analysing the output of f on previously unseen symbols. Although we associate these invariants with our existing understanding of the task to mistakenly anthropomorphise the machine, for example by thinking it has learned $X:mary$ as *someone*, it is important to acknowledge that these are just symbolic patterns. In these cases, our interpretations do not necessarily correspond to any understanding of the machine, relating to the Chinese room argument made by Searle (1980).

Learning invariants by lifting ground examples is related to least common generalisation (Reynolds, 1970) by which inductive inference is performed on facts (Shapiro, 1981) such as generalising $went(mary, kitchen)$ and $went(john, garden)$ to $went(X, Y)$. Unlike in a predicate logic setting, our approach allows for soft alignment and therefore generalisation between varying length sequences. Existing neuro-symbolic systems (Broda et al., 2002) focus on inducing rules that adhere to *given* logical semantics of what a variable and a rule are. For example, δILP (Evans & Grefenstette, 2018) constructs a network by rigidly following the given semantics of first-order logic. Similarly, Lifted Relational Neural Networks (Sourek et al., 2015) ground first-order logic rules into a neural network while Neural Theorem Provers (Rocktschel & Riedel, 2017) build neural networks using backward-chaining (Russell & Norvig, 2016) on a given background knowledge base with templates. This architectural approach for combining logical variables is also observed with Tensor-Log (Cohen, 2016) and Logic Tensor Networks (Serafini & d’Avila Garcez, 2016) while grounding logical rules can also be used as regularisation (Hu et al., 2016). However, the notion of a variable is pre-engineered rather than learned with a focus on presenting a practical approach to solving certain problems whereas our motivation stems from a cognitive perspective.

At first it may seem the learned invariants, Section 6, make the model more interpretable; however, this transparency is not of the model f but of the data. The invariant captures patterns that potentially approximates the data generating distribution but we still do not know *how* the model f uses them upstream. Thus, from the perspective of explainable artificial intelligence (XAI) (Adadi & Berrada, 2018), learning invariants or interpreting them do not constitute an explanation of the reasoning model f even though “if *someone* goes *somewhere* then they are there” might look like one. Instead, it can be perceived as causal attribution (Miller, 2019) in which someone being somewhere is attributed to them going there. This perspective also relates to gradient based model explanation methods such as Layer-Wise Relevance Propagation (Bach et al., 2015) and Grad-CAM (Selvaraju et al., 2017; Chattopadhyay et al., 2018). Consequently, a possible view on ψ , equation 2, is a gradient based usefulness measure such that a symbol utilised upstream by f to determine the answer becomes a variable similar to how a group of pixels in an image contribute more to its classification.

Finally, one can argue that our model maintains a form of counterfactual thinking (Roese, 1997) in which soft unification g creates counterfactuals on the invariant example to alter the output of f towards the desired answer, equation 4. The question where Mary would have gone if Mary had gone to the garden instead of the kitchen is the process by which an invariant is learned through multiple examples during training. This view relates to methods of causal inference (Pearl, 2019; Holland, 1986) in which counterfactuals are vital as demonstrated in structured models by Pearl (1999).

8 CONCLUSION

We presented a new approach for learning variables and lifting examples into invariants through the usage of soft unification. Evaluating on four datasets, we analysed how Unification Networks perform comparatively to existing similar architectures while having the benefit of lifting examples into invariants that capture underlying patterns present in the tasks. Since our approach is end-to-end differentiable, we plan to apply this technique to multi-modal tasks in order to yield multi-modal invariants for example in visual question answering.

ACKNOWLEDGMENTS

We would like to thank Murray Shanahan for his helpful comments, critical feedback and insights regarding this work.

REFERENCES

- Amina Adadi and Mohammed Berrada. Peeking inside the black-box: A survey on explainable artificial intelligence (XAI). *IEEE Access*, 6:52138–52160, 2018. doi: 10.1109/access.2018.2870052.
- Sebastian Bach, Alexander Binder, Grégoire Montavon, Frederick Klauschen, Klaus-Robert Müller, and Wojciech Samek. On pixel-wise explanations for non-linear classifier decisions by layer-wise relevance propagation. *PLOS ONE*, 10(7):e0130140, July 2015. doi: 10.1371/journal.pone.0130140.
- Dzmitry Bahdanau, Kyunghyun Cho, and Yoshua Bengio. Neural machine translation by jointly learning to align and translate. *ICLR*, September 2015.
- Krysia B. Broda, Artur S. D’Avila Garcez, and Dov M. Gabbay. *Neural-Symbolic Learning Systems*. Springer London, 2002. ISBN 1852335122.
- Aditya Chattopadhyay, Anirban Sarkar, Prantik Howlader, and Vineeth N. Balasubramanian. Grad-CAM++: Generalized gradient-based visual explanations for deep convolutional networks. In *2018 IEEE Winter Conference on Applications of Computer Vision (WACV)*, pp. 839–847. IEEE, IEEE, March 2018. doi: 10.1109/wacv.2018.00097.
- Sneha Chaudhari, Gungor Polatkan, Rohan Ramanath, and Varun Mithal. An attentive survey of attention models. *IJCAI*, April 2019.
- Kyunghyun Cho, Bart van Merriënboer, Dzmitry Bahdanau, and Yoshua Bengio. On the properties of neural machine translation: Encoder–decoder approaches. In *Proceedings of SSST-8, Eighth Workshop on Syntax, Semantics and Structure in Statistical Translation*. Association for Computational Linguistics, 2014. doi: 10.3115/v1/w14-4012.
- Nuri Cingillioglu and Alessandra Russo. Deeplogic: Towards end-to-end differentiable logical reasoning. *AAAI-MAKE*, May 2019.
- Keith L. Clark. Negation as failure. In *Logic and Data Bases*, pp. 293–322. Springer US, 1978. doi: 10.1007/978-1-4684-3384-5_11.
- William W. Cohen. Tensorlog: A differentiable deductive database. *arXiv:1605.06523*, 2016.
- Richard Evans and Edward Grefenstette. Learning explanatory rules from noisy data. *Journal of Artificial Intelligence Research*, 61:1–64, January 2018. doi: 10.1613/jair.5714.
- Gottlob Frege. Sense and reference. *The Philosophical Review*, 57(3):209, May 1948. doi: 10.2307/2181485.
- Joe L. Frost, Pei-San Brown, John A. Sutterby, and Candra D. Thornton. *The Developmental Benefits Of Playgrounds*. Association for Childhood Education International, 2004. ISBN 0871731649.
- Alex Graves, Greg Wayne, and Ivo Danihelka. Neural turing machines. *arXiv:1410.5401*, 2014.

- Alex Graves, Greg Wayne, Malcolm Reynolds, Tim Harley, Ivo Danihelka, Agnieszka Grabska-Barwińska, Sergio Gómez Colmenarejo, Edward Grefenstette, Tiago Ramalho, John Agapiou, Adrià Puigdomènech Badia, Karl Moritz Hermann, Yori Zwols, Georg Ostrovski, Adam Cain, Helen King, Christopher Summerfield, Phil Blunsom, Koray Kavukcuoglu, and Demis Hassabis. Hybrid computing using a neural network with dynamic external memory. *Nature*, 538(7626): 471–476, October 2016. doi: 10.1038/nature20101.
- Mikael Henaff, Jason Weston, Arthur Szlam, Antoine Bordes, and Yann LeCun. Tracking the world state with recurrent entity networks. *ICLR*, 2017.
- Paul W. Holland. Statistics and causal inference. *Journal of the American Statistical Association*, 81(396):945–960, December 1986. doi: 10.1080/01621459.1986.10478354.
- Zhiting Hu, Xuezhe Ma, Zhengzhong Liu, Eduard Hovy, and Eric Xing. Harnessing deep neural networks with logic rules. *ACL*, 2016. doi: 10.18653/v1/p16-1228.
- Diederik P. Kingma and Jimmy Ba. Adam: A method for stochastic optimization. *ICLR*, 2015.
- Ankit Kumar, Ozan Irsoy, Peter Ondruska, Mohit Iyyer, James Bradbury, Ishaan Gulrajani, Victor Zhong, Romain Paulus, and Richard Socher. Ask me anything: Dynamic memory networks for natural language processing. In *ICML*, pp. 1378–1387, 2016.
- Richard L. Lewis. Cognitive modeling, symbolic. *The MIT encyclopedia of the cognitive sciences*, pp. 525–527, 1999.
- Zachary C. Lipton. The mythos of model interpretability. *Communications of the ACM*, 61(10): 36–43, September 2018. doi: 10.1145/3233231.
- Fei Liu and Julien Perez. Gated end-to-end memory networks. In *Proceedings of the 15th Conference of the European Chapter of the Association for Computational Linguistics: Volume 1, Long Papers*, pp. 1–10. Association for Computational Linguistics, 2017. doi: 10.18653/v1/e17-1001.
- Thang Luong, Hieu Pham, and Christopher D. Manning. Effective approaches to attention-based neural machine translation. In *Proceedings of the 2015 Conference on Empirical Methods in Natural Language Processing*. Association for Computational Linguistics, 2015. doi: 10.18653/v1/d15-1166.
- Tim Miller. Explanation in artificial intelligence: Insights from the social sciences. *Artificial Intelligence*, 267:1–38, February 2019. doi: 10.1016/j.artint.2018.07.007.
- Adam Morton and Jerry A. Fodor. *The Language of Thought.*, volume 75. Philosophy Documentation Center, March 1978. doi: 10.2307/2025426.
- Stephen Muggleton and Luc de Raedt. Inductive logic programming: Theory and methods. *The Journal of Logic Programming*, 19-20:629–679, May 1994. doi: 10.1016/0743-1066(94)90035-3.
- Judea Pearl. Probabilities of causation: three counterfactual interpretations and their identification. *Synthese*, 121(1-2):93–149, 1999.
- Judea Pearl. The seven tools of causal inference with reflections on machine learning. *Communications of the ACM*, 62(3):54–60, February 2019. doi: 10.1145/3241036.
- Jean Piaget. *The Psychology of Intelligence*. Routledge, August 2001. ISBN 0415254019.
- John C. Reynolds. Transformational systems and algebraic structure of atomic formulas. *Machine intelligence*, 5:135–151, 1970.
- Tim Rocktschel and Sebastian Riedel. End-to-end differentiable proving. *NIPS*, pp. 3791–3803, 2017.
- Neal J. Roese. Counterfactual thinking. *Psychological Bulletin*, 121(1):133–148, 1997. doi: 10.1037/0033-2909.121.1.133.

- Stuart Russell and Peter Norvig. *Artificial Intelligence: A Modern Approach (3rd Edition)*. Pearson, November 2016. ISBN 1292153962.
- John R. Searle. Minds, brains, and programs. *Behavioral and brain sciences*, 3(3):417–424, 1980. doi: 10.1016/b978-1-4832-1446-7.50007-8.
- Ramprasaath R. Selvaraju, Michael Cogswell, Abhishek Das, Ramakrishna Vedantam, Devi Parikh, and Dhruv Batra. Grad-CAM: Visual explanations from deep networks via gradient-based localization. In *2017 IEEE International Conference on Computer Vision (ICCV)*, pp. 618–626. IEEE, October 2017. doi: 10.1109/iccv.2017.74.
- Minjoon Seo, Sewon Min, Ali Farhadi, and Hannaneh Hajishirzi. Query-reduction networks for question answering. *ICLR*, 2017.
- Luciano Serafini and Artur d’Avila Garcez. Logic tensor networks: Deep learning and logical reasoning from data and knowledge. *arXiv:1606.04422*, 2016.
- Ehud Y. Shapiro. *Inductive inference of theories from facts*. Yale University, Department of Computer Science, 1981.
- Gustav Sourek, Vojtech Aschenbrenner, Filip Zelezny, and Ondrej Kuzelka. Lifted relational neural networks. *arXiv:1508.05128*, 2015.
- Sainbayar Sukhbaatar, Arthur Szlam, Jason Weston, and Rob Fergus. End-to-end memory networks. In *NIPS*, pp. 2440–2448, 2015.
- Seiya Tokui, Kenta Oono, Shohei Hido, and Justin Clayton. Chainer: a next-generation open source framework for deep learning. In *Proceedings of Workshop on Machine Learning Systems (LearningSys) in The Twenty-ninth Annual Conference on Neural Information Processing Systems (NIPS)*, 2015. URL http://learningsys.org/papers/LearningSys_2015_paper_33.pdf.
- J. Marshall Unger and Terrence W. Deacon. *The Symbolic Species: The Co-Evolution of Language and the Brain*, volume 82. Wiley, 1998. doi: 10.2307/329984.
- Jason Weston, Sumit Chopra, and Antoine Bordes. Memory networks. *ICLR*, 2015.
- Jason Weston, Antoine Bordes, Sumit Chopra, Alexander M. Rush, Bart van Merrinboer, Armand Joulin, and Tomas Mikolov. Towards ai-complete question answering: A set of prerequisite toy tasks. *ICLR*, 2016.
- Caiming Xiong, Stephen Merity, and Richard Socher. Dynamic memory networks for visual and textual question answering. *ICML*, pp. 2397–2406, 2016.

A MODEL DETAILS

A.1 UNIFICATION MLP & CNN

Unification MLP (UMLP) To model f as a multi-layer perceptron, we take symbol embeddings of size $d = 16$ and flatten sequences of length $l = 4$ into an input vector of size $\phi(\mathbf{k}) \in \mathbb{R}^{64}$. The MLP consists of 2 hidden layers with tanh non-linearity of sizes $2d$ and d respectively. To process the query, we concatenate the one-hot encoding of the task id to $\phi(\mathbf{k})$ yielding a final input of size $64 + 4 = 68$. For unification features ϕ_U , we use a bi-directional GRU with hidden size d and an initial state of $\mathbf{0}$. The hidden state at each symbol is taken with a linear transformation to give $\phi_U(s) = \mathbf{W}_U \Phi(s)$ where $\Phi(s)$ is the hidden state of the biGRU. The variable assignment is then computed as an attention over the according to equation 3.

Unification CNN (UCNN) We take symbols embeddings of size $d = 32$ to obtain an input grid $\phi(\mathbf{K}) \in \mathbb{R}^{3 \times 3 \times 32}$. Similar to UMLP, for each symbol we append the task id as a one-hot vector to get an input of shape $3 \times 3 \times (32 + 4)$. Then f consists of 2 convolutional layers with d filters each, kernel size of 3 and stride 1. We use relu non-linearity in between the layers. We pad the grid with 2 columns and 2 rows to a 5×5 such that the output of the convolutions yield again a hidden output $\mathbf{H} \in \mathbb{R}^{3 \times 3 \times d}$ of the same shape. As the final hidden output h , we take a global max pool to over \mathbf{H} to obtain $\mathbf{h} \in \mathbb{R}^d$. Unification function g is modelled identical to f without the max pooling such that $\phi_U(\mathbf{K}_{ij}) = \mathbf{H}'_{ij}$ where \mathbf{H}' is the hidden output of the convolutional layers.

A.2 UNIFICATION MEMORY NETWORKS

Unlike previous architectures, with UMN we interleave g into f . We use embedding sizes of $d = 32$ and model f with an iterative memory network. We take the final hidden state of a bi-directional GRU, with initial state $\mathbf{0}$, Φ_M to represent the sentences of the context \mathbf{C} and query \mathbf{q} in a d -dimensional vector $\mathbf{M}_i = \Phi_M(\mathbf{C}_i)$ and the query $\mathbf{m}_q = \Phi_M(\mathbf{q})$. The initial state of the memory network is $\mathbf{h}^0 = \mathbf{m}_q$. At each iteration j :

$$\mathbf{A}_i^j = \tanh(\mathbf{W} \rho(\mathbf{M}_i, \mathbf{h}^j) + \mathbf{b}) \quad (6)$$

$$\beta^j = \text{softmax}(\mathbf{W} \Phi_A(\mathbf{A}^j) + \mathbf{b}) \quad (7)$$

where Φ_A is another d -dimensional bi-directional GRU and $\rho(\mathbf{x}, \mathbf{y}) = [\mathbf{x}; \mathbf{y}; \mathbf{x} \odot \mathbf{y}; (\mathbf{x} - \mathbf{y})^2]$ with \odot the element-wise multiplication and $[\cdot]$ the concatenation of vectors. Taking β^j as the context attention, we obtain the next state of the memory network:

$$\mathbf{h}^{j+1} = \sum_i \beta_i^j \tanh(\mathbf{W} \rho(\mathbf{M}_i, \mathbf{h}^j) + \mathbf{b}) \quad (8)$$

and iterate J many times in advance. The final prediction becomes $f(\mathbf{C}, \mathbf{q}) = \text{softmax}(\mathbf{W} \mathbf{h}^J + \mathbf{b})$. All weight matrices \mathbf{W} and bias vectors \mathbf{b} are independent but are tied across iterations.

B GENERATED DATASET SAMPLES

Table 4: Sample context, query and answer triples from sequences and grid tasks.

Dataset	Task	Context	Query	Answer
Sequence	i	1488	constant	2
Sequence	ii	6157	head	6
Sequence	iii	1837	tail	7
Sequence	iv	3563	duplicate	3
Grid	i	0 0 0 0 2 2 8 2 2	box	2
Grid	ii	4 0 0 0 7 0 8 0 1	head	4
Grid	iii	0 6 0 1 7 2 0 3 0	centre	7
Grid	iv	8 0 0 5 6 0 2 4 1	corner	2

Table 5: Training sizes for randomly generated fixed length sequences and grid tasks with 8 unique symbols. The reason for Grid task (i) to be smaller is because there are at most 32 combinations of 2×2 boxes in a 3×3 grid with 8 unique symbols.

Task	Sequences	Grid
i	704.7 ± 12.8	25.6 ± 1.8
ii	709.4 ± 13.8	623.7 ± 14.1
iii	709.7 ± 14.0	768.2 ± 12.5
iv	624.8 ± 12.4	795.2 ± 10.3

C TRAINING DETAILS

C.1 UNIFICATION MLP & CNN

Both unification models are trained on a 5-fold cross-validation over the generated datasets for 2000 iterations with a batch size of 64. We don't use any weight decay and save the training and test accuracies every 10 iterations, as presented in Figure 3.

C.2 UNIFICATION MEMORY NETWORKS

We again use a batch size of 64 and pre-train f for 40 epochs then f together with g for 260 epochs. We use epochs for UMN since the dataset sizes are fixed. To learn g alongside f , we combine error signals from the unification of the invariant and the example. Following equation 4, the objective function not only incorporates the negative log-likelihood \mathcal{L}_{nll} of the answer but also the mean squared error between intermediate states \mathbf{h}_I^j and \mathbf{h}_K^j at each iteration as an auxiliary loss:

$$J = \mathcal{L}_{\text{nll}}(f(K), a) + \lambda_U \left[\mathcal{L}_{\text{nll}}(f \circ g(I, K), a) + \frac{1}{J} \sum_{j=1}^J (\mathbf{h}_I^j - \mathbf{h}_K^j)^2 + \tau \sum_{s \in \mathcal{S}} \psi_w(s) \right] \quad (9)$$

We pre-train by setting $\lambda_U = 0$ for 40 epochs and then set $\lambda_U = 1$. For strong supervision we also compute the negative log-likelihood \mathcal{L}_{nll} for the context attention β^j , described in Appendix A, at each iteration using the supporting facts of the tasks. We apply a dropout of 0.1 for all recurrent neural networks used and only for the bAbI dataset weight decay with 0.001 as the coefficient.

D FURTHER RESULTS

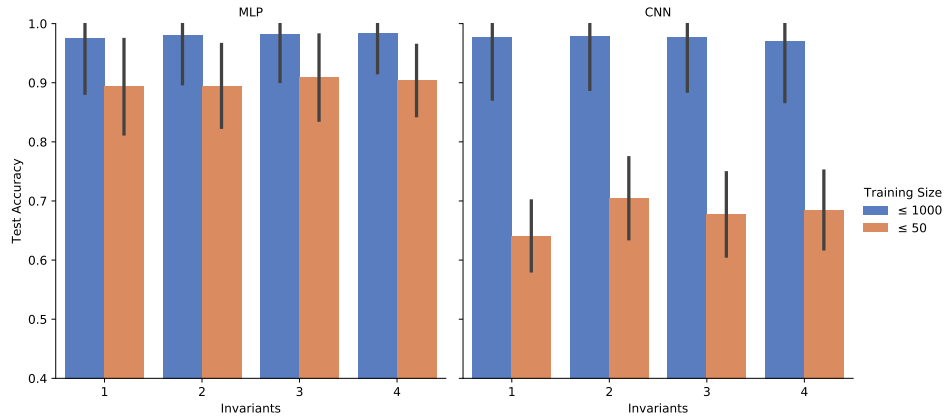


Figure 6: Results of Unification MLP and CNN on increasing number of invariants. There is no impact on performance when more invariants per task are given. Upon closer inspection, we noticed the models ignore the extra invariants and only use 1. We speculate the regularisation ψ encourages the models to use a single 1 invariant.

Table 6: Individual task error rates on bAbI tasks for Unification Memory Networks.

Supervision # Invs Training Size	Weak		Strong		
	1 1k	3 1k	1 1k	3 1k	3 50
1	0.0	0.0	0.0	0.0	1.4
2	65.6	63.1	0.3	0.7	30.0
3	67.1	62.6	1.0	2.4	39.8
4	0.0	0.0	0.0	0.0	37.0
5	3.4	4.0	0.8	1.1	26.5
6	0.2	0.6	0.0	0.0	18.4
7	22.0	22.8	10.7	11.3	22.8
8	10.3	8.5	7.4	7.6	24.7
9	0.1	25.7	0.0	0.0	33.8
10	0.1	2.0	0.0	0.3	32.6
11	0.0	0.0	0.0	0.0	11.9
12	0.0	0.1	0.0	0.0	21.3
13	2.1	3.7	0.0	0.1	5.8
14	19.7	13.5	0.5	0.1	54.8
15	0.0	0.7	0.0	0.0	0.0
16	55.2	56.2	0.0	0.0	39.7
17	39.2	49.0	51.1	49.3	48.8
18	4.4	8.0	0.6	0.5	10.4
19	91.8	89.6	53.9	46.7	90.2
20	0.0	0.0	0.0	0.0	2.7
Mean	19.1	20.5	6.3	6.0	27.6
Std	27.9	27.0	15.6	14.3	21.0
# > 5%	8	10	4	4	17

Table 7: Comparison of individual task error rates (%) on the bAbI (Weston et al., 2016) dataset of the best run. We preferred 1k results if a model had experiments published on both 1k and 10k for data efficiency. References from left to right: (Sukhbaatar et al., 2015) - (Liu & Perez, 2017) - (Henaff et al., 2017) - (Seo et al., 2017) - Ours - (Xiong et al., 2016) - (Graves et al., 2016) - (Weston et al., 2015) - Ours - (Kumar et al., 2016)

Support Size	Weak								Strong		
	Model	N2N	GN2N	1k EntNet	QRN	UMN	10k DMN+	DNC	1k MemNN	UMN	10k DMN
1	0.0	0.0	0.7	0.0	0.0	0.0	0.0	0.0	0.0	0.0	0.0
2	8.3	8.1	56.4	0.5	65.6	0.3	0.4	0.0	0.7	1.8	
3	40.3	38.8	69.7	1.2	67.1	1.1	1.8	0.0	2.4	4.8	
4	2.8	0.4	1.4	0.7	0.0	0.0	0.0	0.0	0.0	0.0	
5	13.1	1.0	4.6	1.2	3.4	0.5	0.8	2.0	1.1	0.7	
6	7.6	8.4	30.0	1.2	0.2	0.0	0.0	0.0	0.0	0.0	
7	17.3	17.8	22.3	9.4	22.0	2.4	0.6	15.0	11.3	3.1	
8	10.0	12.5	19.2	3.7	10.3	0.0	0.3	9.0	7.6	3.5	
9	13.2	10.7	31.5	0.0	0.1	0.0	0.2	0.0	0.0	0.0	
10	15.1	16.5	15.6	0.0	0.1	0.0	0.2	2.0	0.3	2.5	
11	0.9	0.0	8.0	0.0	0.0	0.0	0.0	0.0	0.0	0.1	
12	0.2	0.0	0.8	0.0	0.0	0.0	0.0	0.0	0.0	0.0	
13	0.4	0.0	9.0	0.3	2.1	0.0	0.1	0.0	0.1	0.2	
14	1.7	1.2	62.9	3.8	19.7	0.2	0.4	1.0	0.1	0.0	
15	0.0	0.0	57.8	0.0	0.0	0.0	0.0	0.0	0.0	0.0	
16	1.3	0.1	53.2	53.4	55.2	45.3	55.1	0.0	0.0	0.6	
17	51.0	41.7	46.4	51.8	39.2	4.2	12.0	35.0	49.3	40.6	
18	11.1	9.2	8.8	8.8	4.4	2.1	0.8	5.0	0.5	4.7	
19	82.8	88.5	90.4	90.7	91.8	0.0	3.9	64.0	46.7	65.5	
20	0.0	0.0	2.6	0.3	0.0	0.0	0.0	0.0	0.0	0.0	
Mean	13.9	12.7	29.6	11.3	19.1	2.8	3.8	6.7	6.0	6.4	
# > 5%	11	10	15	5	8	1	2	4	4	2	

Table 8: Individual task error rates (%) on the logical reasoning dataset.

Support Size	1k				10k						50	20k	
	Weak		Strong		Weak		Strong		Strong			Weak	
Arity	1	2	1	2	1	2	1	2	2	2		2	2
# Invs / Model	1	3	1	3	1	3	1	1	3	3		DMN	IMA
Facts	1.2	0.9	0.0	0.4	0.0	0.0	0.0	0.0	0.0	33.5	0.0	0.0	
Unification	0.0	10.3	0.0	10.8	0.0	0.0	0.0	0.0	0.0	41.3	13.0	10.0	
1 Step	50.3	49.8	4.4	20.0	1.2	27.8	0.1	1.3	5.7	50.2	26.0	2.0	
2 Steps	47.5	50.0	5.7	35.0	37.2	47.8	0.0	29.7	28.7	49.9	33.0	5.0	
3 Steps	47.6	49.2	10.4	38.7	39.6	45.6	0.0	26.0	26.1	48.3	23.0	6.0	
AND	31.3	37.4	10.7	16.4	29.8	29.0	0.2	0.4	1.2	50.0	20.0	5.0	
OR	25.2	38.1	21.0	35.0	20.5	30.2	4.4	20.6	17.4	47.6	13.0	3.0	
Transitivity		50.0		26.6		39.6		5.0	6.0	49.2	50.0	50.0	
1 Step NBF	46.4	38.7	3.8	28.8	1.1	21.6	0.1	1.1	8.0	47.6	21.0	2.0	
2 Steps NBF	48.5	48.9	7.7	39.6	30.4	48.2	0.1	33.4	28.7	50.3	15.0	4.0	
AND NBF	51.0	50.1	43.1	48.6	29.4	44.2	0.1	1.3	40.1	49.5	16.0	8.0	
OR NBF	51.4	48.4	50.8	47.3	47.6	47.8	21.3	27.6	30.5	47.3	25.0	14.0	
Mean	36.4	39.3	14.3	28.9	21.5	31.8	2.4	12.2	16.0	47.1	21.2	9.1	
Std	18.7	15.9	16.4	14.1	17.1	16.7	6.1	13.2	13.6	4.7	12.3	13.4	
# > 5%	9	11	7	11	7	10	1	5	9	12	11	5	

$$\frac{\frac{X\text{sandra went back to the } Y\text{:bathroom}}{\text{is } X\text{:sandra in the } Y\text{:bathroom}}}{\text{yes}}$$

Figure 7: bAbI task 6, yes or no questions. The invariant does not variablise the answer.

$$\begin{aligned} X:m (Y:e) &\vdash X:m (Y:e) \\ X:a (Y:w , Z:e) &\vdash X:a (Y:w , Z:e) \\ X:m (\top) &\vdash X:m (c) \\ X:x (A) \leftarrow \text{not } Z:q (A) &\vdash X:x (Y:z) \end{aligned}$$

Figure 8: Invariants learned on tasks 1, 2 and 11 with arity 1 and 2 from the logical reasoning dataset. Last invariant on task 11 lifts the example around the negation by failure, denoted as *not*, capturing its semantics.

3 X 7 Y head	X 0 0 0 Y 0 6 4 Y
7 4 X Y head	0 1 0 1 X 8 0 X 8
X 3 1 X tail	0 0 Y 0 2 0 0 0 7
X X 5 Y duplicate	head centre corner

(a) Invariants with extra variabes learned with UMLP. (b) Mismatching invariants learned with UCNN.

Figure 9: Invariants learned that do not match the data generating distribution from UMLP and UCNN using ≤ 1000 examples to train. In these instances the unification still bind to the the correct symbols in order to predict the desired answer; quantitatively we get the same results. Variable default symbols are omitted for clarity.